Cyclones enhance the transport of sea spray aerosols to the high atmosphere in the Southern Ocean

Jun Shi[1,2], Jinpei Yan*[1,2], Shanshan Wang[1,2], Shuhui Zhao[3], Miming Zhang[1,2], Suqing Xu[1,2], Qi Lin[1,2], Hang Yang[1,2], Siying Dai[1,2]

[1]Key Laboratory of Global Change and Marine Atmospheric Chemistry, Ministry of Natural Resources, Xiamen 361005, China;

[2]Third Institute of Oceanography, Ministry of Natural Resources, Xiamen 361005, China.

[3]School of Tourism, Taishan University, Tai'an City, Shandong Province, 271000, China.

***Corresponding author：**

Jinpei Yan, Phone: 86-592-2095920, E-mail: jpyan@tio.org.cn

Address: No. 178 Daxue Road, Siming District, Xiamen City, Fujian Province, China

Abstract： Cyclones are expected to increase the vertical transport of sea spray aerosols (SSAs), which may significantly impact the climate by increasing cloud condensation nuclei (CCN) and cloud droplets (N_d) population. In this study, a high-time resolution (1h) aerosol monitoring was carried out in the mid- and high Southern Hemisphere from 23th February 2018 to 4th March 2018. The characteristics of SSAs during three cyclones were observed in the cruise. The results showed that SSAs level in the low atmosphere didn't increase with the wind speed during cyclone processes, which was different from the anticipated scenario that SSAs concentration increased with wind speed. However, the size of SSA particles during cyclones was larger than that in the no-cyclone periods. It seems that the generation of SSAs was enhanced during cyclones, but SSAs concentration near the sea surface increased scarcely. The upward transport proportion was calculated according to the wind stress and sea-salt flux between cyclone and non-cyclone periods. It indicated that more than 23.4% of the SSAs were transported upward by cyclone processes during Event 1, and 36.2% and 38.9% in Event 2 and Event 3, respectively. The upward transport of SSAs was the main reason why SSAs concentration didn't increase in the low atmosphere. The transport of SSAs to the high atmosphere during cyclones may increase the CCN burden additionally in the marine boundary layer, which may affect the regional climate. This study highlights the importance of SSAs transport to the high atmosphere by cyclone and extends the knowledge of SSAs generation and impact factor during the cyclone period in marine atmosphere.

Keywords: Sea spray aerosols (SSAs); Cyclone; Southern Ocean (SO); Transport

1. Introduction

Sea spray aerosols (SSAs) were one of the largest sources of primary aerosols in the marine atmosphere, making a significant contribution to aerosols in the marine atmosphere (McInnes et al., 1996). It is reported that the annual global SSAs flux was estimated to be 1.01 × 10^4Tg yr^{-1} (Gong et al., 2002). Pure sea salt mostly consisted of NaCl and a mixture of one or more other salts, such as Mg, K, Ca, sulfates and traces of organic materials (Thomas et al., 2022). SSAs were considered to be the most important contributor to aerosol light scattering in the marine boundary layer (MBL) (Quinn and Coffman, 1999; Takemura et al., 2002). In addition, as the source of cloud condensation nuclei (CCN), SSAs can alter solar radiation reflection, extent the lifetime of clouds and further impact the global climate (Pierce and Adams, 2006). The influence of SSAs on cloud properties was thought to be particularly intense over remote ocean region devoid of continental particles. Studies have found that The largest SSA CCN number fractions, up to 65%, were observed in the high southern latitudes (40◦ S to 70◦ S) at low supersaturation (0.1%) (Quinn et al., 2017).

SSAs are generated predominantly by the action of wind on the ocean (Stokes et al., 2013) as the major mechanism of SSAs production is bubble bursting at sea surface as a result of wind stress (Monahan and Muircheartaigh, 1980). Wind stress on the sea surface forms waves. Then bubbles are generated and return to the sea surface, creating whitecaps. Subsequently, the bubble bursts and jets droplets into the atmosphere. Hence, the sea salt particle size and concentration of SSAs was significantly depended on the wind speed (McDonald et al., 1982). However, some studies have showed that wind speed was not the sole impact factor of SSAs production, as humidity, temperature and sea-air temperature would also impact SSAs generation (Cole et al., 2003; Shi et al., 2022; Liu et al., 2020). The generation of SSAs in the marine atmosphere have been investigated in previous studies, but the production of SSAs during extreme weather (such as cyclones) in the mid- and high Southern Hemisphere is still lack of knowledge.

Westerlies in the Southern Hemisphere fundamentally control regional patterns of air temperature and also regulate ocean circulation, heat transport and carbon uptake (Goyal et al., 2021). Moreover, the zone of westerlies is prone to cyclones which dominate the precipitation pattern of the mid- and high Southern Hemisphere (Mycoy et al., 2020). Southern Ocean (SO) plays an important role in global carbon cycles and climate changes (Gruber et al., 2019). Furthermore, the SO is scarcely affected by human activities, in which the influence of SSAs on CCN is particularly strong in this region.

Cyclones may carry large water volumes and impose strong winds, which have a significant impact on marine aerosols, especially on SSAs. (Fang et al., 2009). Air convergence due to the reduction of pressure caused by cyclones may also affect SSAs concentration. Typically, higher frequency of cyclone was developed during the summer season than in other seasons. It is reported that 959 cyclones occurred in the SO during summer time from 2004 to 2008 (Liu et al., 2012).

In summary, the impact of cyclones on the emission of SSAs can't be ignored. SSAs can direct absorbing and scattering of solar radiation. Additionally, sea spray aerosol is an important source of CCN, which plays a significant role in regulating global warming, but it remains unclear that how does the cyclone impact SSAs emission. Cyclones developing in the westerlies and SO result in the decrease of pressure, air convergence, strong winds and heavy precipitation, which alter the emission of SSAs and thus affects regional climate in the mid- and high latitudes of the Southern Hemisphere. However, the lack of direct observations makes it challenge to deep insight into this question. Generally, the observation of cyclones is commonly performed at fixed points on land

(Badarinath et al., 2008), but such observations cannot be used to investigate the effect of cyclones on SSAs over remote ocean regions. However, high-time resolution observation technology is now available on research vessels to carried out the SSAs monitoring and understand the SSAs behavior during cyclone processes.

In this study, SSAs characteristics were observed with high-time resolution during three cyclones in the SO to determine the transport of SSAs to the high atmosphere by cyclones. The concentration and particle size of SSAs were measured simultaneously for the first time with high-time resolution (1h) in the mid- and high Southern Hemisphere from 23th February to 4th March 2018. The results provide a new insight into the effect of cyclones on the generation and vertical transport of SSAs in the mid- and high latitudes of the Southern Hemisphere.

2. Methodology

2.1 Observational sites

Observations were carried out on board the R/V "Xuelong" during the 34th Chinese Antarctica Expedition Research Cruise from 23th February and 4th March 2018. The observation covered with a large portion of the SO (40°S to 73°S, 170°E to 124°W, seen in Fig. S1).

2.2 SSAs measurement

Aerosol composition was monitored with a temporal resolution of 1 h using an in-situ gas and aerosol composition monitoring system (IGAC, Model S-611 http://www.machine-shop.com.tw/). To minimize the impact of ship emissions, the sampling inlet connected to the monitoring instruments was fixed on a mast (20 m above the sea surface) located at the bow of the research vessel. Note that the major pollutants were from the chimney, which is located at the stern of the

R/V and about 25 meters above the sea level. Hence, the pollution emissions from the vessel mainly located at the downwind of the sampling inlet, especially when the vessel is running forward. As high-time-resolution observations were used in this study, the self-contaminations from the vessel have been eliminated from the measurement results. The wind speed and wind directions were also monitoring during the observation period, which were used to determine if the observations were affected by the self-contaminations or not. A total suspended particulate sample inlet was also positioned at the top of the mast. All aerosol observational instruments were connected by conductive silicone tubing with an inner diameter of 1.0 cm.

The IGAC monitoring system consisted of three main units, including a Wet Annular Denuder (WAD), a Scrub and Impact Aerosol Collector (SIAC) and an ion chromatograph with a sampling flow of 16.7 LPM. The collection of acidic and basic gases relies on the diffusion and absorption of gases into a downward flowing aqueous solution. The SIAC was positioned at an angle to facilitate the collection of enlarged particles. Ultrapure water was fed continuously into the nozzle at 1.2 $mL.min^{-1}$ and heated to 140 °C to generate stream, which was sprayed directly towards the particle-laden air to improve the humidity of flue gases. Fine particles were enlarged and subsequently accelerated through a conical-shaped impaction nozzle and collected on the impaction plate. The gas and aerosol liquid samples from the WAD and SIAC were drawn separately by a pair of syringe pumps. The samples were then analyzed for anions and cations by an online ion chromatography (IC) system (Dionex ICS-3000). The injection loop size was 500μL for both anions and cations (Young et al., 2016). Six to eight concentrations of standard solutions were used for calibration purposes, depending on the target concentration (R^2 values above 0.997). The detection limits for Na^+ concentration was 0.03 μg. L^{-1} (aqueous solution).

2.3 SSA particle size measurement

A single particle mass spectrometer (SPAMS) was used to measure the SSAs particle size distribution. A nafion tube dryer was placed at the inlet of SPAMS to remove the moisture of sampling gas. Details of the methods used for aerosol detection and the operational procedure for the on-board SPAMS have been described carefully in the previous study (Li et al., 2014). The performance of particle size distribution determination using SPAMS has been confirm (Yan et al., 2016; Li et al., 2014; Ma et al; 2016). A $PM_{2.5}$ collector was deployed to remove particles larger than 2.5 μm. Fine particles were drawn into the vacuum system through a critical orifice and then accelerated and focused to form a particle beam. Particles with specific velocities then passed through two Nd: YAG lasers (532 nm). The aerodynamic diameter of single particle was calculated by the particle velocity. The particle size detected by the SPAMS was calibrated using polystyrene latex spheres (PSL, Duke Scientific Corp., Palo Alto) with diameter of 0.2, 0.3, 0.5, 0.75, 1.0, 2.0, and 2.5 μm (Li et al., 2011).

2.4 Meteorological parameters

Meteorological parameters such as wind speed (WS), wind direction and temperature etc. were measured continuously using an automated meteorological station mounted on the R/V “Xuelong". Weather map data, including sea surface pressure and total precipitation, was obtained from the fifth generation ECMWF reanalysis for the global climate and weather (ERA5. https://cds.climate.copernicus.eu/). Satellite cloud maps were obtained from the Level-1 and Atmosphere Archive and Distribution System Distributed Active Archive Center (LAADS DAAC data product MOD021KM. https://ladsweb.modaps.eosdis.nasa.gov/).

2.5 Undisturbed SSA concentration estimates during the cyclone period

Undisturbed SSAs (U-SSAs) is defined as the SSAs generation supposed without cyclone impact in the marine boundary layer during the cyclone process, which was determined by the wind stress and sea-salt flux. The upward transport proportion of SSA was estimated by comparing U-SSA concentration with the concentration of SSAs during cyclone period. U-SSA concentration during the cyclone period were estimated in two ways as follow.

The momentum flux at the air-sea interface, also called wind stress, is an important part of the interaction between ocean and atmosphere, which reflects the friction and drag effect between the two fluids. Wind stress is the energy source of SSAs generation. The momentum flux at the air-sea interface can be calculated using the following equation (Toffoli et al., 2012):

$$\tau = \rho_a C_d U_{10}^2 \quad (1)$$

Where, ρ_a is the air density, U_{10} is the wind speed measured at 10 m above the sea surface, and C_d is a drag coefficient, which can be expressed as follow:

$$C_d=(a+bU_{10})\times 10^{-3} \quad (2)$$

Where, a is 0.96 and b is 0.06.

According to the difference of wind stress between cyclonic and non-cyclonic periods, combining with the concentration of SSAs during non-cyclonic periods, U-SSA $_{\text{(wind stress)}}$ concentration can be obtained.

$$\text{U-SSA}_{\text{(wind stress)}}=\frac{\tau_{\text{cy}}}{\tau_{\text{non-cy}}}*\text{SSA}_{\text{(non-cy)}} \quad (3)$$

For the indirect production of SSAs through the formation and bursting of bubbles, the SSAs flux function dF_0/d_r (particles m^{-2} s^{-1} mm^{-1}) which expresses the rate of sea water droplet generation per unit area of sea surface per increment of particle radius, is given by Monahan et al. (1986) as

Eq. (4):

$$\text{SSA flux} = \frac{dF_0}{dr} = 1.373 U_{10}^{3.41} r^{-3} (1+0.057 r^{1.05}) \times 10^{1.19 e^{-B^2}} \quad (4)$$

Where, $B = (0.38 - \log r)/0.65$, r is the particle radius.

Then, U-SSA $_{\text{(Sea-salt flux)}}$ concentration can be obtained as follow:

$$\text{U-SSA}_{\text{(Sea-salt flux)}} = \frac{\text{SSA flux}_{\text{cy}}}{\text{SSA flux}_{\text{non-cy}}} * \text{SSA}_{\text{(non-cy)}} \quad (5)$$

3. Results and discussion

3.1 Meteorology and cyclone events

The observation region in the SO was defined by the outermost closed isobar surrounding the cyclone area center (Wernli and Schwierz, 2006). Rainfall has numerous aspects impact of SSAs production. Generally, raindrops falling onto the sea surface can produce SSA particles directly or indirectly, either from bubbles entrained by the drop or SSA particles produced by the splashed drops (Blanchard and Woodcock, 1957). However, raindrops can also function as efficient scavenger of particles in the atmosphere (Lewis and Schwartz, 2004). Hence, the precipitation period was extracted, when the transport of SSAs by cyclones was discussed in this study. As known that relative humidity also has an impact on SSAs, high relative humidity was presented in this study, which basically reached the deliquescence point (about RH:75%) of NaCl (Cole et al, 2003). In this case, the change of relative humidity has little effect on the particle size. Three cyclone events were observed during the cruise (Fig. S2). Na^+ derived from SSAs is an important component of marine atmospheric aerosols (Teinila et al., 2014) and is generally considered to be a marker of SSAs in the marine atmosphere (Yeatman et al., 2001). Hence, the relationship between Na^+ concentrations and meteorological factors were discussed in this study, seen in Fig. 1.

The first cyclone was generated in the mid- Southern Hemisphere (45°S, 150°E), and gradually moved to eastwards (Fig. 2). As the cyclone approached, the R/V "Xuelong" sampled a northwest warm and humid air mass followed by precipitation. As the research vessel entered the cyclone area (Event 1. shadow area in Fig. 1) at about 15:00 24/2/18 (UTC time), air pressure suddenly dropped from 1003 hpa to 961 hpa and wind speed significantly enhanced, comparing with the non-cyclone area (average wind speed increased from 11.7 m s^{-1} to 14.8 m s^{-1}). However, the average Na^+ concentration during this cyclone event remained relatively constant as the WS increased, changing from 1529 ng m^{-3} to 1706 ng m^{-3}. At about 23:00 25/2/18, the research vessel left the cyclone area. Note that wind speed dropped sharply between 13:00 and 23:00 25/2/18 (average wind speed decreased from 14.8 ms^{-1} to 9.3 ms^{-1}) and this was matched by a rapid decrease in SSAs concentration (from 1706 ng m^{-3} to 343 ng m^{-3}, seen in Fig. 1b).

The vessel encountered another cyclone area at 10:00 26/2/18 and immediately turned to the southeast, leaving the cyclone area at 22:00 26/2/18 (Event 2, seen in Fig. 1). During Event 2, the research vessel did not pass through the center of the cyclone. However, it was also affected by the cyclone, as the atmospheric pressure dropped from 983 hpa to 973 hpa and the average wind speed increased from 13.5 m s^{-1} to 15.5 m s^{-1}. Similar to Event 1, the average Na^+ concentration during the cyclone period remained relatively constant, or even decreased from 2810 ng m^{-3} to 2354 ng m^{-3}, as the WS increased. During the event 2, the dominant air flow was cold and westerly thus there was only a little precipitation (Fig. 2).

While the research vessel moved southeast and arrived at sea ice edge of the high SO, Na^+ concentration was much lower than the value during the first two cyclone events, which suggested that low air temperature and sea ice coverage reduced SSAs generation (Fig. S3) (Yan et al., 2020). Between 18:00 1/3/18 and 04:00. 4/3/18, the research vessel encountered the third cyclone (Event

3). Wind speed increased from 7.5 m s^{-1} to 21.5 m s^{-1} and the air pressure dropped from 986 hpa to 960 hpa (lowest). Similarly, the average Na^+ concentration during this cyclone period showed little increase (changing from 255 ng m^{-3} to 335 ng m^{-3}). The third cyclone was relatively stable and moved slowly, but the cyclone only brought a small amount of precipitation in the wind shear region.

3.2 SSA properties during cyclone processes

Correlation coefficients between different compositions of sea spray aerosols in the atmospheric were shown in Table S1. Na^+ correlated well with Mg^{2+}, K^+, Ca^{2+} and SO_4^{2-}, implying Na^+ has a good representation of SSAs. The variation of Na^+ concentrations in different latitude regions is presented in Fig. S4. Positive correlations between Na^+ concentrations and wind speeds were found in the low-middle latitudes (20°S - 40°S) (R=0.59, Fig.S4), where the atmospheric pressure remained stable (Fig. S5). This suggests that that SSAs generation was greatly influenced by the wind speed. However, the correlation between Na^+ concentrations and wind speed was relatively low in middle-high latitudes (40°S-60°S) and in the polar region (60°S-74°S) (R=0.45 and 0.05, respectively), where unstable atmosphere state or cyclone occurred frequency in these areas (Fig. S5), suggesting that cyclone may affect the relationship between wind speed and SSAs concentration in the marine atmosphere.

The relationship between WS and Na^+ concentration in different meteorological conditions are illustrated in Fig. 3. To further investigate the influence of the cyclone on SSA concentrations in the mid- and high Southern Hemisphere, a non-cyclone period (April 5th and 6th) with stable pressure and relative humidity but without precipitation, was selected as a control period (defined as normal period).

It is readily apparent that Na^+ concentrations and SSAs increased with the WS during the control period (Fig. 3a, R = 0.74). Positive correlations between Na^+ concentrations and WS were also presented during non-cyclone effects in event 1, event 2 and event 3 (R = 0.65, 0.64 and 0.50, respectively, seen in Fig. 3b, 3c and 3d), which was in good agreement with previous study (O'Dowd and de Leeuw, 2007). It is worth noting that the correlation between Na^+ concentration and WS during Event 3 were lower than the value during the other two cyclone events. This was caused by the low temperature and sea ice coverage in the high SO, which weakened the influence of WS on SSA generation (Yan et al., 2020).

In contrast, poor correlations between Na^+ concentration and wind speed were found during all the three cyclone periods (R = -0.32, 0.15 and 0.44) and precipitation periods (R = 0.08 and -0.02. Fig. 3b, 3c and 3d). During the cyclone periods, Na^+ concentration changed irregularly as the WS increased, suggesting that rainfall altered the effect of wind stress on SSA generation. The effect of precipitation on the formation of SSA was complicated and WS may not be the critical factor that affected SSAs emission during precipitation process. Further studies of how does precipitation affect SSAs are required.

It is interesting that an obvious correlation between WS and Na^+ concentration was not presented during cyclone process with high wind speed. Na^+ concentration during cyclone periods was even lower than those during non-cyclone periods. That means the generation of SSAs did not enhanced during the cyclone process or the SSAs was transported by the cyclone. The generation and transport of SSAs during cyclone process was further discussed in the following section.

3.3 SSA particle size distribution

Generally, SSA generation increased with wind speed, however in this study it was found that higher wind speed did not result in higher levels of SSAs during cyclone process. It seems that the generation of SSAs was suppressed during cyclone. It is necessary to determine whether the emission of SSAs in the cyclonic periods was higher than that in the non-cyclone periods. Feng et al. (2017) and Liu et al. (2020) reported that both SSAs particle size and the concentration increased with increasing wind speed. As the WS increased from 3.4 to 10 m s^{-1}, a 7–10 fold increase in atmospheric sea salt concentration was observed. Log-normal distributions predicted a 30-fold increase in the concentration (μg/m^3) of particles larger than 1 x 10^{-9} g (10 μm radius) and a 50-fold increase in the concentration of particles larger than 1 x 10^{-8} g (20 μm radius) (McDonald et al., 1982). If the particle size of SSAs increased with increasing wind speed, it indirectly confirmed that the concentration of SSAs also increase.

The size distributions of SSAs observed during the three cyclone events are presented in Table S2 and Fig. 4. During Event 1, the difference between the number of SSA particles larger than 1.2 μm observed in cyclone and non-cyclone periods was about 11%. The change of SSA size distribution during Event 2 and Event 3 were consistent with that during Event 1 (about 6% and 5%, respectively). The mean size of SSA particles was larger during cyclone period than that during no-cyclone period. These results revealed that cyclones in mid- and high Southern Hemisphere enhanced SSAs generation. However, the increase of SSAs concentration was not presented as expected when high wind speed occurred during cyclone period, suggesting that SSAs may be transported or diluted in the lower atmosphere.

3.4 Estimation of the upward transport proportion of SSAs by cyclone

The mid- and high latitude of Southern Hemisphere, especially in the Antarctic region is one of the most pristine in the world and serves as an important proxy for the pre-industrial atmosphere, which was less affected by human activity. Hence, anthropogenic aerosols account for a small proportion of the total aerosol population. In the SO, aerosols are typically derived from natural sources, including primary particles (sea spray and bursting bubbles), which make up the vast majority of the aerosol mass. In this region cyclones tend to occur in summer, generating more SSAs due to high WS. The observation results suggested that air convergence caused by the cyclone may result in considerable quantities of SSAs being transported vertically to high atmosphere, which can partly explain why the mean number concentration of CCN/cloud droplets (N_d) in the SO in summer is much higher than that in winter (Mycoy et al., 2020).

As mentioned above, the size of SSAs was larger during cyclone events than that in no-cyclone period. However, the level of SSAs in the low atmosphere hardly increased with wind speed during the cyclone process. It’s likely that considerable SSAs were transported upward by air convergence due to cyclone. When large number of SSAs were transported to the upper air, the SSAs in high atmosphere enhanced solar radiation reflected back to space by modulating the N_d, which in turn changed cloud reflectivity even without any changes of cloud macrostructure (Twomey, 1977). Furthermore, cloud microphysical processes were also altered with changing CCN/N_d (Albrecht, 1989). These two effects, summarized in Fig. 5, can ultimately affect the radiation balance of the earth system in the mid- and high latitudes of Southern Hemisphere (Quinn and Bates, 2011). Thus the effect of cyclone on SSAs generation, especially in the polar region, can’t be neglected.

It is difficult to precisely estimate the proportion of SSAs transported vertically directly.

However, the differences of wind stress and sea-salt flux between cyclone and non-cyclone periods can be used to calculate the undisturbed concentrations of Na^+ (U-SSA concentration) during the cyclone period. This can be used to quantify the upward transport proportion of SSAs.

Fig. S6 and S7 show the differences of wind stress and sea-salt flux between cyclone and non-cyclone periods. The estimated proportion of vertically transport of SSAs, using the wind stress method and the sea-salt flux method, are presented in Table 1. According to the calculation results, more than 23.4% of the SSAs were transported upward by cyclone process during Event 1, and 36.2% and 38.9% in Event 2 and Event 3, respectively. The upward transport proportion of SSAs estimated using the bubble method were higher than those estimated using the wind stress method for all the three cyclone events. As the research vessel was located at the high SO and close to the Antarctica during Event 3, the upward transport proportion estimated using the bubble method was the highest, reaching 56.6%, which was much higher than the results estimated for Event 1 (39.9%) and Event 2 (42.8%).

The high transportation ratio in Event 3 was agree well with the results of previous study which reported that the largest contribution of SSAs to CCN (up to 65%) was observed in the high southern latitudes (Quinn et al., 2017). Another factor affecting the estimated result in Event 3 was that R/V "Xuelong" located at the high SO. As the sea state was typically not fully developed in such a situation, the energy flux from the air to the ocean may differ from that under steady state conditions, which may affect wave breaking and SSAs production (Lewis and Schwartz, 2004). These circumstances can lead to the overestimation of vertical transport proportion of SSAs. In summary, the results suggested that in the mid- and high the Southern Hemisphere, a significant proportion of SSAs was transported upward and subsequently potentially affected regional climate change.

The influence of cyclone on SSAs in the tropics, characterized by stronger and more intricate cyclonic system, was not covered by this paper. Further studies of how does SSAs concentration change in the tropical cyclone area are required. However, the observational results presented in this study extend the current knowledge of the impact of cyclone on marine aerosol emission in the mid- and high Southern Hemisphere and their potential climate effect.

Conclusions

An underway aerosol monitoring system was used to determine the aerosol composition and size distribution during different cyclone events in the mid- and high Southern Hemisphere in order to access the potential effects of cyclone on SSAs emission. Three cyclone events were observed during the 34th Chinese Antarctica Expedition Research Cruise from 23th February 2018 to 4th March 2018.

It was expected that the high wind speeds produced during the cyclone events would increase the generation of SSAs. However, the SSAs levels increase in the low atmosphere were not observed during these cyclone events. It indicated that considerable SSAs were transported upward to the high atmosphere due to the cyclone. According to the wind stress and sea-salt flux between cyclone and non-cyclone periods, the calculation indicated that more than 23% of SSAs were transported upwards to the high atmosphere, with the highest proportion observed in the Southern Ocean (ranging from 39% to 55%). Vertical transport of SSAs can be regarded as an important source of CCN in the marine boundary layer.

The effect of cyclone on SSAs emission was indirect and complicated. Therefore, future work is required to investigate the effect of varying intensity of the cyclone on SSAs emission and SSAs generation mechanism during precipitation, as well as their potential climate effect in different regions.

Acknowledgements

This study is financially supported by the Qingdao National Laboratory for Marine Science and Technology (No. QNLM2016ORP0109), the Natural Science Foundation of Fujian Province, China (No. 2019J01120), the Response and Feedback of the Southern Ocean to Climate Change (RFSOCC2020-2025), the Chinese Projects for Investigations and Assessments of the Arctic and Antarctic (CHINARE2017-2020), and the National Natural Science Foundation of China (No. 41941014). The authors gratefully acknowledge the Guangzhou Hexin Analytical Instrument Company Limited for on-board observation technical assistance, and the Zhangjia Instrument Company Limited for IGAC technical assistance and data analysis.

Data availability

The data discussed in this manuscript are available from the following websites: https://doi.org/10.5281/zenodo.7912911.

Author contributions.

SJ analyzed the results and wrote the paper. JY conducted the observations, proposed the research ideas and wrote the paper. SW and SZ contributed considerably to the interpretation of the results. MZ and QL conducted the on-board observations and data analyses. SX applied the calculations of sea ice distribution and Metrological data. HY and SD contributed to the observation data analyses.

Competing interests

The authors declare that they have no conflict of interest.

References

Albrecht, B. A: Aerosols, Cloud Microphysics, and Fractional Cloudiness. Science, 245(4923), 1227–1230, https://doi.org/10.1126/science.245.4923.1227, 1989.

Badarinath, K. V. S., Kharol, S. K., Krishna Prasad, V., Kaskaoutis, D. G., and Kambezidis, H. D.: Variation in aerosol properties over Hyderabad, India during intense cyclonic conditions. International Journal of Remote Sensing, 29(15), 4575-4597,https://doi.org/10.1080/01431160801950170. 2008.

Blanchard, D.C., and A.H. Woodcock.: Bubble formation and modification in the sea and its meteorological significance, Tellus,9,145-158,https://doi.org/10.3402/tellusa.v9i2.9094, 1957.

Cole, I. S., Paterson, D. A., and Ganther, W. D.: Holistic model for atmospheric corrosion Part 1 - theoretical framework for production, transportation and deposition of marine salts. Corrosion Engineering, Science and Technology, 38(2), 129–134,.https://doi.org/10.1179/147842203767789203, 2003.

Fang, G., Lin, S., Chang, S., Chou, C.: Effect of typhoon on atmospheric particulates in autumn in central Taiwan. Atmos. Environ. 43, 6039e6048,https://doi.org/10.1016/j.atmosenv.2009.08.033, 2009.

Feng, L., Shen, H., Zhu, Y., Gao, H., and Yao, X.: Insight into Generation and Evolution of Sea-Salt Aerosols from Field Measurements in Diversified Marine and Coastal Atmospheres. Scientific Reports, 7(1). https://doi:10.1038/srep41260, 2017.

Fu, H. Y., Zheng, M., Yan, C. Q., Li, X. Y., Gao, H. W., Yao, X. H., Guo, Z., and Zhang, Y. H.: Sources and characteristics of fine particles over the Yellow Sea and Bohai Sea using online single particle aerosol mass spectrometer. Journal of Environmental Sciences, 29, 62–70,https://doi.org/10.1016/j.jes.2014.09.031, 2015.

Goyal, R., Sen Gupta, A., Jucker, M., and England, M. H.: Historical and projected changes in the Southern Hemisphere surface westerlies. Geophysical Research Letters, 48(4), e2020GL090849,https://doi.org/10.1029/2020GL090849, 2021

Gong, S. L., Barrie, L. A., and Lazare, M.: Canadian Aerosol Module (CAM): A size-segregated simulation of atmospheric aerosol processes for climate and air quality models 2. Global sea-salt aerosol and its budgets. Journal of Geophysical Research: Atmospheres, 107(D24),https://doi.org/10.1029/2001jd002004, 2002.

Gruber, N., Landschutzer, P., and Lovenduski, N. S.: The variable Southern Ocean carbon sink. Annual Review of Marine Science, 11(1), 159,https://doi.org/10.1146/annurev-marine-121916-063407, 2019.

Jiang, B., Xie, Z., Lam, P. K. S., He, P., Yue, F., Wang, L., Huang, Y., Kang, H., Yu, X.,and Wu, X.: Spatial and temporal distribution of sea salt aerosol mass concentrations in the marine boundary layer from the Arctic to the Antarctic. Journal of Geophysical Research: Atmospheres, 126(6), e2020JD033892,https://doi.org/10.1029/2020JD033892. 2021.

Lewis, E. R., and Schwartz, S. E.: Sea salt aerosol production: Mechanisms, methods, measurements, and models. American Geophysical Union,413 pp, ISBN:9780875904177, 2004.

Li, L., Huang, Z., Dong, J., Li, M., Gao, W., Nian, H., Fu, Z., Zhang, G., Bi, X., Cheng, P., and Zhou, Z.: Real time bipolar time-of-flight mass spectrometer for analyzing single aerosol particles. Int. J. Mass Spectrom. 303(2-3), 118e124,https://doi.org/10.1016/j.ijms.2011.01.017, 2011.

Li, L., Li, M., Huang, Z., Gao, W., Nian, H., Fu, Z., Gao, J., Chai, F., Zhou,Z., Ambient particle characterization by single particle aerosol mass spectrometry in an urban area of Beijing. Atmos Environ94,323–331, https://doi.org/10.1016/j.atmosenv.2014.03.048, 2014.

Liu, N., Fu, G., and Kuo, Y.-H.: Statistical characteristics of austral summer cyclones in Southern Ocean. Journal of Ocean University of China, 11(2), 118-128,https://doi:10.1007/s11802-012-1828-7, 2012.

Liu, S., Liu, C.-C., Froyd, K. D., Schill, G. P., Murphy, D. M., Bui, T. P., Dean-Day, J. M., Weinzierl, B., Dollner, M., Diskin, G. S., Chen, G., and Gao, R.-S.: Sea spray aerosol concentration modulated by sea surface temperature, P. Natl. Acad. Sci. USA, 118, e2020583118, https://doi.org/10.1073/pnas.2020583118, 2021.

Ma, L., Li, M., Zhang, H., Li, L., Huang, Z., Gao, W., Chen, D., Fu, Z., Nian, H., Zou, L., Gao, J., Chai, F., and Zhou, Z. :Comparative analysis of chemical composition and sources of aerosol particles in urban Beijing during clear, hazy, and dusty days using single particle aerosol mass spectrometry. Journal of Cleaner Production, 112, 1319–1329,https://doi.org/10.1016/j.jclepro.2015.04.054 2016.

McDonald, R. L., Unni, C. K., and Duce, R. A. Estimation of atmospheric sea salt dry deposition: Wind speed and particle size dependence. Journal of Geophysical Research, 87(C2), 1246,https://doi.org/10.1029/JC087iC02p01246, 1982.

McInnes, L. M., Quinn, P. K., Covert, D. S. and Anderson, T. L.: Gravimetric analysis, ionic composition, and associated water mass of the marine aerosol. *Atmos. Environ.* 30, 869–884, https://doi.org/10.1016/1352-2310(95)00354-1, 1996.

McCoy, I. L., McCoy, D. T., Wood, R., Regayre, L., Watson-Parris, D., Grosvenor, D. P., Mulcahy, J. P., Hu, Y., Bender, F. A.-M., Field, P. R., Carslaw, K. S., and Gordon, H.: The hemispheric contrast in cloud microphysical properties constrains aerosol forcing, P. Natl. Acad. Sci. USA, 117, 18998–19006, https://doi.org/10.1073/pnas.1922502117, 2020.

Monahan, E. C., and Muircheartaigh, I. O.: Optimal power-law description of oceanic whitecap coverage dependence on wind-speed. Journal of Physical Oceanography, 10(12), 2094–2099, https://doi.org/10.1175/1520-0485(1980)010<2094:Opldoo>2.0.Co;2, 1980.

Monahan, E. C., Spiel, D. E., and Davidson, K. L.: Oceanic whitecaps and their role in air-sea exchange, chap. A model of marine aerosol generation via whitecaps and wave disruption, pp. 167–174, D. Reidel, Norwel, Mass. ISBN: 978-90-277-2251-5, 1986.

O'Dowd, C. D., & de Leeuw, G.: Marine aerosol production: A review of the current knowledge. Philosophical Transactions of the Royal Society A: Mathematical, Physical and Engineering Sciences, 365(1856), 1753–1774, https://doi.org/10.1098/rsta.2007.2043, 2007.

Pierce, J. R., andAdams, P. J.: Global evaluation of CCN formation by direct emission of sea salt and growth of ultrafine sea salt. Journal of Geophysical Research, 111(D6), D06203, https://doi.org/10.1029/2005jd006186, 2006.

Quinn, P. K. and Coffman, D. J.; Comment on “Contribution of different aerosol species to the global aerosol extinction optical thickness: estimates from model results” by Tegen et al. J. Geophys. Res. 104, 4241–4248, https://doi.org/10.1029/1998JD200066, 1999.

Quinn, P. K., and Bates, T. S.: The case against climate regulation via oceanic phytoplankton sulphur emissions. *Nature*, 480(7375), 51–56,https://doi.org/10.1038/nature10580, 2011.

Quinn, P. K., Coffman, D. J., Johnson, J. E., Upchurch, L. M., and Bates, T. S.; Small fraction of marine cloud condensation nuclei made up of sea spray aerosol. Nature Geoscience, 10(9), 674–679, https://doi.org/10.1038/ngeo3003, 2017.

Shi, J., Yan, J., Wang, S., Zhao, S., Zhang, M., Xu, S., Lin, Q. and Yang, H. Determinant of sea salt aerosol emission in the Southern Hemisphere in summer time. Earth and Space Science, *9*(11), https://doi.org/10.1029/2022ea002529, 2022.

M. D. Stokes, G. B. Deane, K. Prather, T. H. Bertram, M. J. Ruppel, O. S. Ryder, J. M. Brady, and D. Zhao.: A marine aerosol reference tank system as a breaking wave analogue for the production of foam and sea-spray aerosols. Atmospheric Measurement Techniques, 6(4), 1085–1094, https://doi.org/10.5194/amt-6-1085-2013, 2013.

Takemura, T., Nakajima, T., Dubovik, O., Holben, B. N., and Kinne, S.: single-scattering albedo and radiative forcing of various aerosol species with a global three-dimensional model. Journal of Climate, 15(4), 333–352, https://doi.org/10.1175/1520-0442(2002)015<0333:ssaarf>2.0.co;2, 2002.

Teinila, K., Frey, A., Hillamo, R., Tulp, H. C., and Weller, R.:A study of the sea-salt chemistry using size-segregated aerosol measurements at coastal Antarctic station Neumayer. Atmospheric Environment, 96, 11–19, https://doi.org/10.1016/j.atmosenv.2014.07.025, 2014.

Twomey, S.: The Influence of Pollution on the Shortwave Albedo of Clouds. Journal of the Atmospheric Sciences, 34(7), 1149–1152, https://doi.org/10.1175/1520-0469(1977)034<1149:tiopot>2.0.co;2, 1977.

Thomas, M. A., Devasthale, A., and Kahnert, M.: Marine aerosol properties over the Southern Ocean in relation to the wintertime meteorological conditions. Atmospheric Chemistry and Physics, 22(1), 119–137, https://doi.org/10.5194/acp-22-119-2022, 2022.

Toffoli, A., Loffredo, L., Le Roy, P., Lefèvre, J.-M., &Babanin, A. V.: On the variability of sea drag in finite water depth. Journal of Geophysical Research: Oceans, 117(C11), https://doi.org/10.1029/2011jc007857 , 2012.

Xu, G. J., Gao, Y., Lin, Q., Li, W., and Chen, L. Q.: Characteristics of water-soluble inorganic and organic ions in aerosols over the Southern Ocean and coastal East Antarctica during austral summer. Journal of Geophysical Research: Atmospheres, 118(23), 13303–13318, https://doi.org/10.1002/2013jd019496, 2013.

Yan, J., Chen, L., Lin, Q., Zhao, S., and Zhang, M.: Effect of typhoon on atmospheric aerosol particle pollutants accumulation over Xiamen, China. Chemosphere, 159, 244–255, https://doi.org/10.1016/j.chemosphere.2016.06.00, 2016.

Yan, J. P., Chen, L. Q., Lin, Q., Zhao, S. H., Li, L., and Zhu, D. Y.: Marine aerosol using on- board aerosol mass spectrometry. Environmental Science, 38(7), 2629–2636, https://doi.org/10.13227/j.hjkx.201612065. 2017.

Yan, J., Jung, J., Lin, Q., Zhang, M., Xu, S., and Zhao, S.: Effect of sea ice retreat on marine aerosol emissions in the Southern Ocean, Antarctica. Science of the Total Environment, 745, 140773, https://doi.org/10.1016/j.scitotenv.2020.140773, 2020.

Yeatman, S. G., Spokes, L. J., and Jickells, T. D.: Comparisons of coarse-mode aerosol nitrate and ammonium at two polluted coastalsites. Atmospheric Environment, 35(7), 1321–1335, https://doi.org/10.1016/S1352-2310(00)00452-0, 2001.

Young, L. H., Li, C. H., Lin, M. Y., Hwang, B. F., Hsu, H. T., Chen, Y. C., Jung, C. R., Chen, K. C., Cheng, D. H., Wang, V. S., Chiang, H. C., Tsai, P. J.:. Field performance of a semi-continuous monitor for ambient PM2.5 water-soluble inorganic ions and gases at a suburban site. Atmospheric Environment, 144, 376–388, https://doi.org/10.1016/j.atmosenv.2016.08.062, 2016.

Figures/Tables

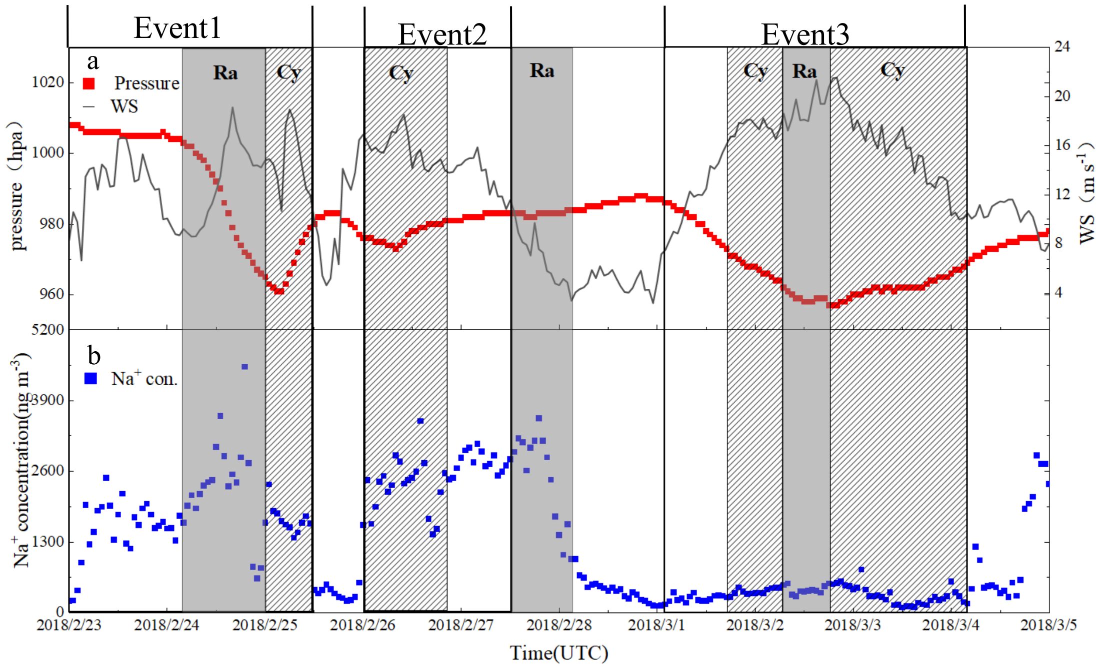

Figure 1. Temporal distributions of Na^+ and relevant meteorological parameters obtained during the period 23 February to 4 March 2018 in the cyclone area of the Southern Ocean. (a) Time series of atmospheric pressure (hpa) and wind speed (WS. m s^{-1}). (b) Time series of Na^+ concentrations (ng m^{-3}). Shading indicates: Ra - precipitation periods; Cy - cyclone periods. No shading corresponds to non-cyclone periods.

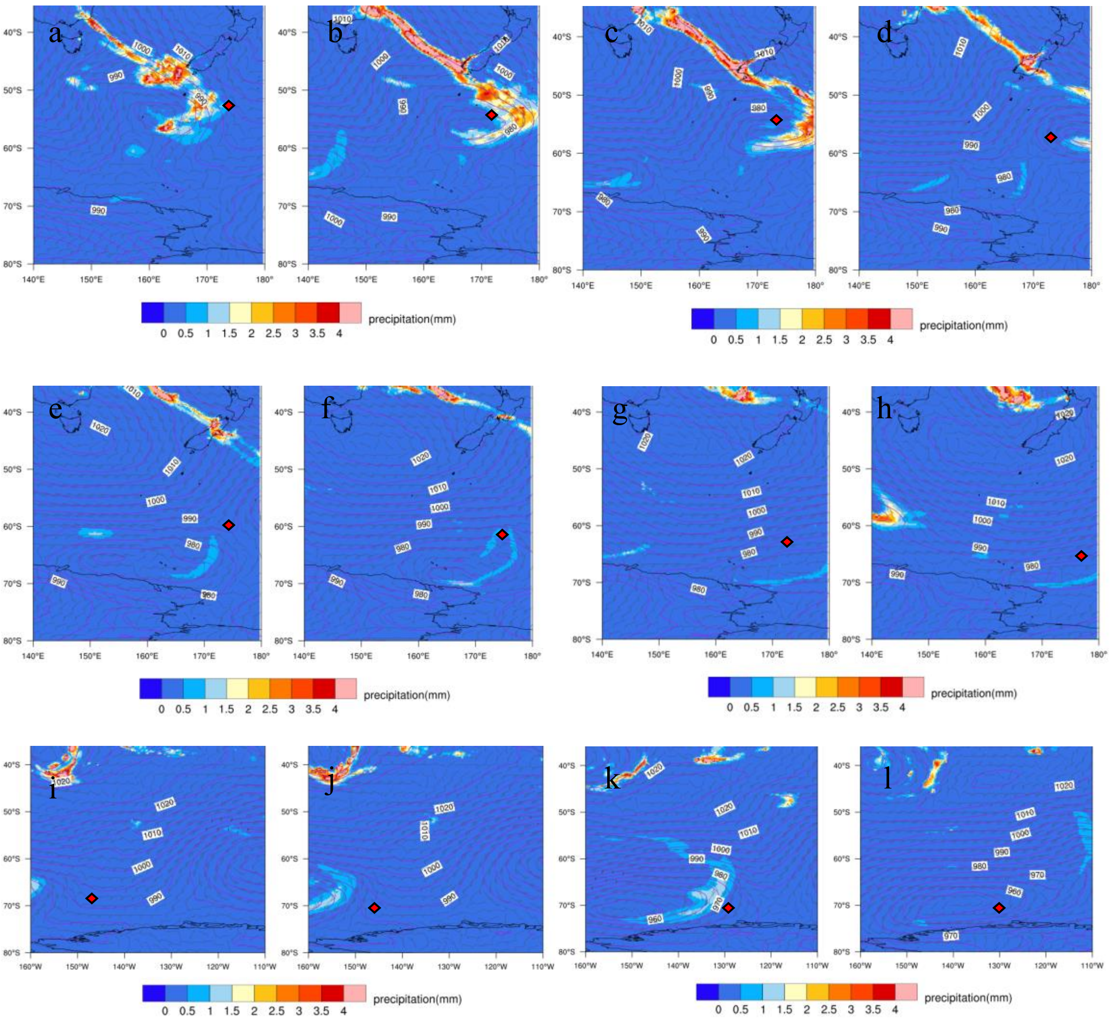

Figure 2. Sea surface pressure (hpa) and total precipitation (mm) maps for the three observed cyclone events. Event 1: (a) 14:00 24/2/18; (b) 20:00 24/2/18; (c) 01:00 25/2/18; (d) 08:00 25/2/18. Event 2: (e) 16:00 25/2/18; (f) 00:00 26/2/18; (g) 20:00 26/2/18; (h) 18:00 26/2/18. Event 3: (i) 01:00 1/3/18 (j) 18:00 1/3/18 (k) 13:00 2/3/18; (l) 22:00 2/3/18. The red diamond represents the position of the research ship. All times are UTC. The coastline of Antarctica is seen at the bottom of each figure.

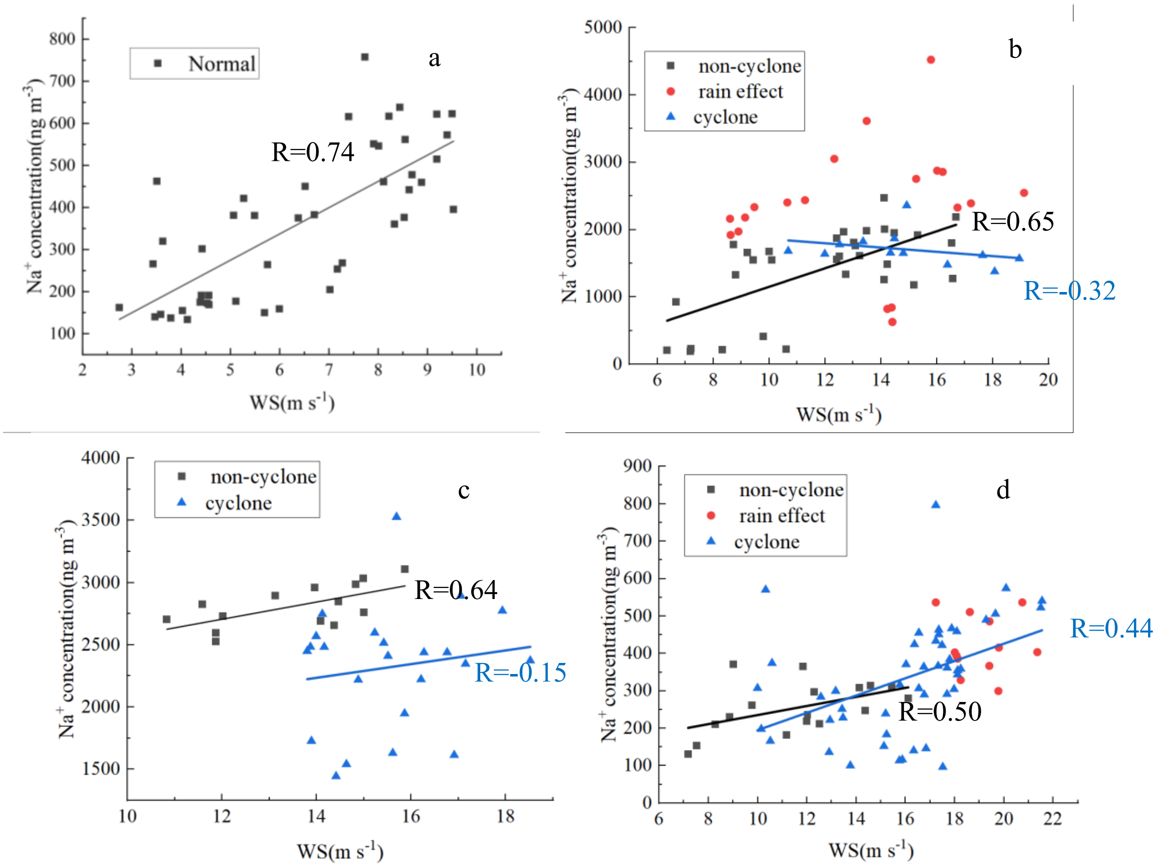

Figure 3. Correlation between Na^+ concentration and wind speed under different meteorological conditions. (a) A non-cyclone "normal" period (i.e., stable air pressure and relative humidity, constant air mass, no precipitation). (b) Event 1 (cyclone, non-cyclone and raining periods). (c) Event 2 (cyclone and non-cyclone periods). (d) Event 3 (cyclone, non-cyclone and raining periods).

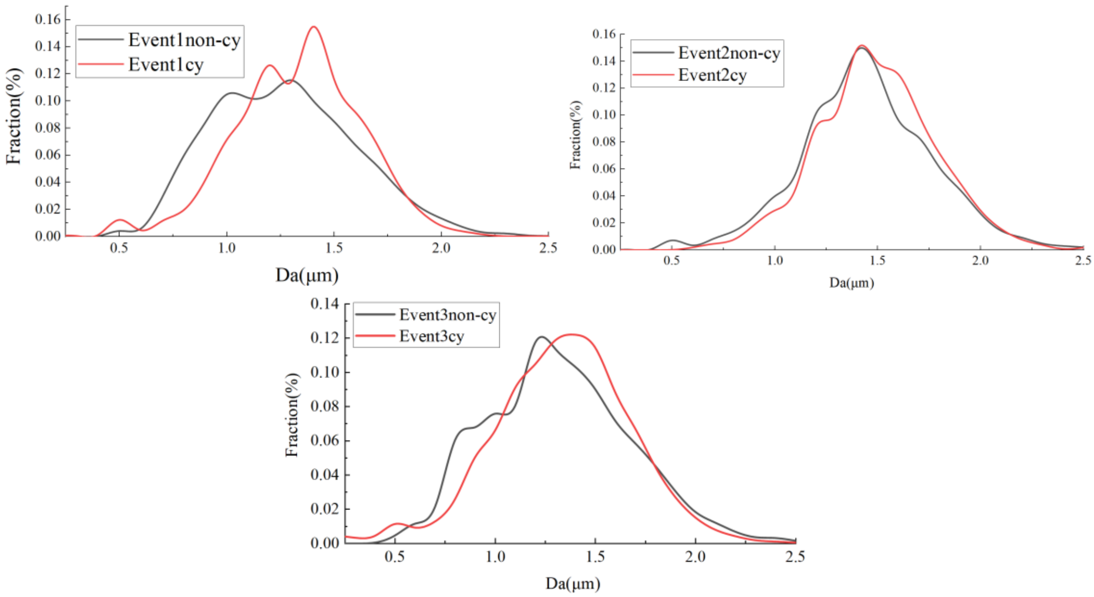

Figure 4. SSA size distributions (in terms of fractional percent) for cyclone and non-cyclone periods during the three observed Events.

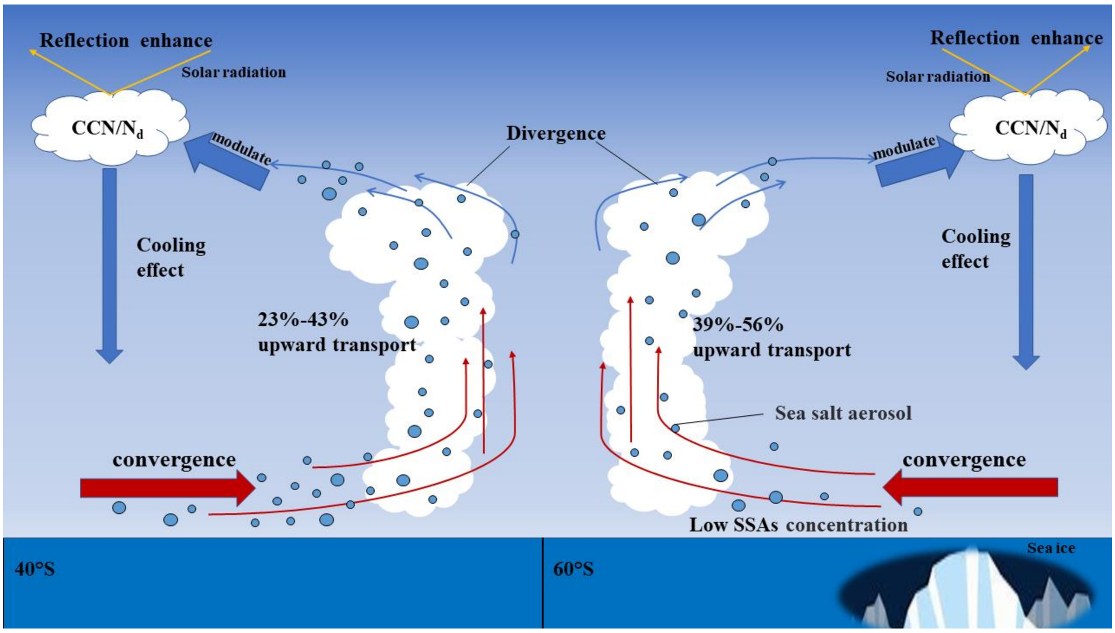

Figure 5. Schematic diagram illustrating the impact of cyclone on SSA generation and transport and the resulting climate effects.

Table 1. Estimation of SSAs vertical transport proportion by assessing the difference of wind stress and Sea-salt flux.

	Event 1	Event 2	Event 3
Quotient of wind stress	1.689	1.310	2.153
Quotient of sea-salt flux	2.156	1.463	3.031
Average Na^+con. (non-cy) ng/m^3	1273.19	2816.90	254.76
Average Na^+con. (cy) ng/m^3	1647.31	2353.74	334.94
Estimated U-$SSA_{(wind\ stress)}$con. ng/m^3	2151.05	3689.30	548.52
Estimated U-$SSA_{(Sea\text{-}salt\ flux)}$con. ng/m^3	2745.16	4113.74	772.14
Estimated upward transport $_{(wind\ stress)}$	23.4%	36.2%	38.9%
Estimated upward transport $_{(Sea\text{-}salt\ flux)}$	39.9%	42.8%	56.6%